PROGRESS REPORT & PROPOSED WORK
Cooperative Agreement No. NCC2-5127

Technical Monitor: Mr. Eugene Tu

Project title: Development of Continuous and Discrete Approaches for Aerodynamic Sensitivity Analysis

Principal Investigator:
Dr. Aditi Chattopadhyay
Associate Professor
Department of Mechanical and Aerospace Engineering
Arizona State University

Co-Principal Investigator:
Dr. Johnny R. Narayan
Research Scientist
Aerospace Research Center
Arizona State University

Graduate Student:
Mr. Wensheng Xu
Department of Mechanical and Aerospace Engineering
Arizona State University

Development of Continuous and Discrete Approaches for Aerodynamic Sensitivity Analysis

Objectives:

The main objectives of the present research were as follows.

(a) Comparison of continuous and discrete semi-analytical design sensitivity techniques for multidisciplinary aircraft optimization problems using comprehensive analysis procedures.

(b) Validation of the two techniques using wing design optimization problems in terms of CPU efficiency and overall nature of the optimum solution.

A comparative study of discrete and continuous semi-analytical sensitivity analysis techniques for evaluating aerodynamic sensitivities in optimization procedures involving CFD solvers for accurate and detailed flow solutions, was proposed. Although there is extensive literature on the discrete and continuous approaches for calculating aerodynamic sensitivities, a study of the relative efficiencies of the approaches has not been performed. This study is crucial in selecting an appropriate sensitivity analysis technique for large scale, multidisciplinary design optimization problems using comprehensive analysis procedures. The study will compare the accuracy and computational efficiency of the two techniques using representative model optimization problems. The nature of the optimum solutions and the computational time (CPU hours) required for arriving at optimum designs are also of interest.

The purpose of the present research is to extend the ongoing effort on semi-analytical sensitivity analysis techniques by performing this important comparative study of the two techniques. The proposed study will compare the accuracy and computational efficiency of the two techniques using representative model optimization problems. The nature of the optimum solutions and the CPU time required for convergence will also be of interest. Finally, parallelization of the developed sensitivity analysis procedures is proposed to improve the computational efficiency and the adaptability to a variety of CFD solvers.

The designs obtained from optimization procedures strongly depend on the accuracy of the analysis procedures that are coupled. An accurate solution of the flow field necessitates the use of accurate Computational Fluid Dynamics (CFD) techniques. Although accurate detailed analyses of many complex flow fields associated with practical engineering systems are now possible, viscous-compressible flow simulations of aircraft configurations can require several CPU hours per steady-state solution. Therefore, the use of such comprehensive procedures for design optimization can be prohibitively expensive when used within a gradient-based optimization technique. Sensitivity analysis, in which the derivative of a system performance function (e.g., the

drag-to-lift ratio of an aircraft wing) with respect to a design variable (e.g., a parameter associated with the wing planform) is calculated, is an essential ingredient in most design optimization procedures. Semi-analytical sensitivity analysis techniques are slowly replacing the traditional finite difference approach because of their efficiency and accuracy. Two popular techniques are the *direct differentiation* approach and the *adjoint variable* approach. In both the techniques, the actual governing equations are differentiated with respect to the design variables using chain rule. The direct differentiation approach yields a large system of equations involving the desired sensitivities which can be solved directly. In the adjoint variable approach, adjoint variables are obtained as the solution to an adjoint problem. The adjoint variables are then used to calculate the sensitivities. These two techniques are equivalent and yield identical results for the sensitivities. If the governing equations are differentiated prior to their discretization, then the semi-analytical approach is categorized as the *continuous sensitivity* approach. In this approach, the sensitivities are calculated using a numerical algorithm similar to the one used for obtaining the flow solution. Therefore, the continuous sensitivity approach needs to be modified, depending upon the governing equations that are differentiated. In the discrete sensitivity approach, the discretized governing algebraic equations are differentiated. Though there is a need for solving a large system of equations here, this procedure can easily be adapted to different analysis procedures. A brief description of the discrete sensitivity analysis is given in Appendix A. The semi-analytical sensitivity analysis techniques are widely used in structural sensitivity calculations and, more recently, have been used for calculating aerodynamic sensitivities.

Milestones:

The major milestones associated with the current research are as follows.

1) Develop an efficient continuous sensitivity analysis procedure
2) Implement the procedure in the appropriate CFD code (UPS3D)
3) Compare the results with discrete sensitivity analysis approach in a relevant problem
4) Modify the procedure to be compatible with parallel processing codes

Research Accomplished (Year-1)

A continuous sensitivity analysis procedure has been completed already (milestone (1)). A reference configuration based approach has been followed to develop this continuous sensitivity analysis procedure. Implementation of the procedure in the UPS3D code (milestone (2)) is underway. This part of the research effort will be completed in about a month (February '96). The strategy is to utilize most of the computational algorithms already existing in the code by configuring the governing equations for the sensitivities similar to those for the flow field. This minimizes development cost, computational resources required in a realistic optimization and makes the procedure more portable to other similar CFD codes. Effort is also underway to carry out milestone (3) in a rigorous manner. This might require minor modifications to the procedure to make it comparable in structure to the discrete sensitivity analysis procedure (already developed and in use for sonic boom minimization related problems) so that a true comparison of the two procedures can be carried out. The continuous sensitivity analysis procedure that has been developed is described below.

Continuous sensitivity analysis:

In the continuous sensitivity approach, the flow variables sensitivities are calculated by directly differentiating the governing partial differential equations. This results in a set of partial differential equations for the sensitivities of the flow variables which are solved using numerical procedures similar to those used in solving the flow equations. In the present work, a continuous sensitivity analysis approach based on the reference configuration has been developed for evaluating the flow variables sensitivities in a multiobjective optimization procedure for high speed flows. Brief description of this development is given below.

The governing equation in integral form is:

$$\frac{\partial}{\partial t}\int_V U dV + \int_S (\overline{\overline{H}} \bullet \vec{n}) dS = 0 \qquad (1)$$

For steady flow, equation (1) becomes:

$$\int_S (\overline{\overline{H}} \bullet \vec{n}) dS = 0 \qquad (2)$$

where

$$\overline{\overline{H}} = (E_i - E_v)i + (F_i - F_v)j + (G_i - G_v)k$$

with

$$\begin{aligned}
E_i &= \left[\rho u, \rho u^2 + p, \rho uv, \rho uw, (E_t + p)u\right]^T \\
F_i &= \left[\rho v, \rho uv, \rho v^2 + p, \rho vw, (E_t + p)v\right]^T \\
G_i &= \left[\rho w, \rho uw, \rho vw, \rho w^2 + p, (E_t + p)w\right]^T \\
E_v &= \left[0, \tau_{xx}, \tau_{xy}, \tau_{xz}, u\tau_{xx} + v\tau_{xy} + w\tau_{xz} - q_x\right]^T \\
F_v &= \left[0, \tau_{xy}, \tau_{yy}, \tau_{yz}, u\tau_{xx} + v\tau_{xy} + w\tau_{xz} - q_y\right]^T \\
G_v &= \left[0, \tau_{xz}, \tau_{yz}, \tau_{zz}, u\tau_{xx} + v\tau_{xy} + w\tau_{xz} - q_z\right]^T \\
E_t &= \rho\left[e + \frac{1}{2}(u^2 + v^2 + w^2)\right]
\end{aligned} \tag{3}$$

The initial configuration is used as the reference configuration. The parameters and variables associated with the reference configuration are identified by an *overbar* in this report. When the design variables change during optimization, a new physical configuration results. Assuming q is design variable vector and $\bar{q}$ is the design variable vector associated with the reference configuration, the transformation equation from the reference configuration to current physical configuration is represented by

$$X(x_1, x_2, x_3) = f(q, \bar{q}, \bar{x}_1, \bar{x}_2, \bar{x}_3) \tag{4}$$

where the subscripts 1-3 represent the coordinate directions for the given system.

The continuous sensitivities can be obtained by differentiating the governing equation (Eqn. 2) using reference configuration as

$$\frac{d}{d\phi_i}\int_S (\overline{\overline{H}} \bullet \vec{n}) dS = 0 \tag{5}$$

Changing the basis of differentiation from the physical configuration to reference configuration, Eqn. (5) can be written as

$$\frac{d}{d\phi_i}\int_{\bar{S}} (\overline{\overline{H}} \bullet \vec{n}) \overline{J_\Gamma} d\bar{S} = \int_{\bar{S}} \left[\frac{d(\overline{\overline{H}} \bullet \vec{n})}{d\phi_i} \overline{J_\Gamma^j} + (\overline{\overline{H}} \bullet \vec{n}) \frac{d\overline{J_\Gamma^j}}{d\phi_i}\right] d\bar{S} = 0 \tag{5a}$$

where

$$\overline{J_\Gamma^j} = \overline{J_\Gamma}\sqrt{\left(\frac{\partial \bar{x}_j}{\partial x_1}\overline{n_j}\right)^2 + \left(\frac{\partial \bar{x}_j}{\partial x_2}\overline{n_j}\right)^2 + \left(\frac{\partial \bar{x}_j}{\partial x_3}\overline{n_j}\right)^2} \tag{6}$$

$$\overline{J_\Gamma} = \det\begin{bmatrix} \partial x_1/\partial \bar{x}_1 & \partial x_1/\partial \bar{x}_2 & \partial x_1/\partial \bar{x}_3 \\ \partial x_2/\partial \bar{x}_1 & \partial x_2/\partial \bar{x}_2 & \partial x_2/\partial \bar{x}_3 \\ \partial x_3/\partial \bar{x}_1 & \partial x_3/\partial \bar{x}_2 & \partial x_3/\partial \bar{x}_3 \end{bmatrix} \tag{7}$$

In the above, $\overline{n_j}$ (i=1,2,3) are the outward normal components of the reference surface $\overline{\Gamma}$. Further differentiation of equation (5a) gives

$$\int_{\bar{S}}\left[\left(\frac{\partial \overline{\overline{\overline{H}}}}{\partial Q^*}\frac{\partial Q^*}{\partial \phi_i}\right)\overline{J_\Gamma^j} + \overline{\overline{\overline{H}}}\frac{d\overline{J_\Gamma^j}}{d\phi_i}\right]\bullet \vec{n}d\bar{S} = 0 \tag{8}$$

where Q^* is the flow variables vector. From Equations (4), (6) and (7), we can solve for $\overline{J_\Gamma^j}$ and $\frac{d\overline{J_\Gamma^j}}{d\phi_i}$. Assuming

$$\overline{\overline{G}} = \left(\frac{\partial \overline{\overline{\overline{H}}}}{\partial Q^*}\frac{\partial Q^*}{\partial \phi_i}\right)\overline{J_\Gamma^j} + \overline{\overline{\overline{H}}}\frac{d\overline{J_\Gamma^j}}{d\phi_i}$$

equation (8) becomes

$$\int_{\bar{S}}(\overline{\overline{G}}\bullet\vec{n})d\bar{S} = 0 \tag{8a}$$

Equation (8a) can now be used in conjunction with the computational algorithm of the CFD code to compute the flow variable sensitivities $\frac{\partial Q^*}{\partial \phi_i}$.

The sensitivities of the performance coefficients of the aircraft to the relevant geometric parameters are calculated as described below. In general, a performance coefficient, C_j, depends on the steady-state flow variables, Q^*, the vector of computational grid coordinates, X, and, sometimes, explicitly on the vector of independent design variables, q. Mathematically this can be stated as,

$$C_j = C_j(Q^*(q), X(q), q) \tag{9}$$

The derivative of C_j with respect to the i^{th} design variable, ϕ_i, is expressed as follows.

$$\frac{dC_j}{d\phi_i} = \left\{\frac{\partial C_j}{\partial Q^*}\right\}^T\left\{\frac{\partial Q^*}{\partial \phi_i}\right\} + \left\{\frac{\partial C_j}{\partial X}\right\}^T\left\{\frac{\partial X}{\partial \phi_i}\right\} + \frac{\partial C_j}{\partial \phi_i} \tag{10}$$

In equation (10), the terms $\left\{\frac{\partial C_j}{\partial Q^*}\right\}$, $\left\{\frac{\partial C_j}{\partial X}\right\}$ and $\frac{\partial C_j}{\partial \phi_i}$ are easily calculated knowing the explicit dependence of C_j on Q^*, X and ϕ_i. Similarly, the grid sensitivities, $\left\{\frac{\partial X}{\partial \phi_i}\right\}$, can be evaluated since the explicit dependence of the physical grid on the design variables (geometric parameters defining the vehicle configuration) is known. Then equation (10) can be solved for the sensitivities of the performance coefficients thus completing the sensitivity analysis. Appendix A describes the optimization problem, the associated analyses and the geometric configuration of the high speed problem addressed.

Grid Sensitivities:

The term $\left\{\frac{\partial X}{\partial \phi_i}\right\}$, which appears in Eqn. 10, represents the grid sensitivity vector. The vector X comprises a set of xyz values corresponding to each point $\xi\eta\zeta$ in the computational grid. In general, a three dimensional hyperbolic grid generation code generates a two-dimensional grid at various stations along the longitudinal direction by solving the following equations.

$$\frac{\partial y}{\partial \eta}\frac{\partial y}{\partial \zeta} + \frac{\partial z}{\partial \eta}\frac{\partial z}{\partial \zeta} = 0 \tag{11}$$

$$\frac{\partial y}{\partial \eta}\frac{\partial z}{\partial \zeta} - \frac{\partial z}{\partial \eta}\frac{\partial y}{\partial \zeta} = F(\eta,\zeta) \tag{12}$$

In Eqn. 12, $F(\eta,\zeta)$ is a known function approximating the Jacobian of transformation between the xyz and the $\xi\eta\zeta$ coordinate systems. Equations 11 and 12 are discretized and solved numerically to obtain the grid vector X. The grid sensitivity vector, $\left\{\frac{\partial X}{\partial \phi_i}\right\}$, can be obtained by directly differentiating Eqns. 11 and 12 with respect to ϕ_i, as follows.

$$\frac{\partial \frac{dy}{d\phi_i}}{\partial \eta}\frac{\partial y}{\partial \zeta} + \frac{\partial y}{\partial \eta}\frac{\partial \frac{dy}{d\phi_i}}{\partial \zeta} + \frac{\partial \frac{dz}{d\phi_i}}{\partial \eta}\frac{\partial z}{\partial \zeta} + \frac{\partial z}{\partial \eta}\frac{\partial \frac{dz}{d\phi_i}}{\partial \zeta} = 0 \tag{13}$$

$$\frac{\partial \frac{dz}{d\phi_i}}{\partial \eta}\frac{\partial y}{\partial \zeta} + \frac{\partial z}{\partial \eta}\frac{\partial \frac{dy}{d\phi_i}}{\partial \zeta} - \frac{\partial \frac{dy}{d\phi_i}}{\partial \eta}\frac{\partial z}{\partial \zeta} - \frac{\partial y}{\partial \eta}\frac{\partial \frac{dz}{d\phi_i}}{\partial \zeta} = \frac{dF}{d\phi_i} \tag{14}$$

Equations 13 and 14, represent a system of equations which can be solved readily to yield the grid sensitivity vector, $\left\{\frac{\partial X}{\partial \phi_i}\right\}$. These equations can be solved using either a continuous or a discrete sensitivity approach.

Proposed Research (Year-2)

The following objectives, derived on the basis of milestones 3 & 4, are proposed for the second year of this research grant. Comparison of the continuous sensitivity analysis with discrete analysis and parallelization of the sensitivity analysis procedure are the two tasks proposed.

1) Validation & Application of Continuous Sensitivity Analysis Procedure:

The flow variable sensitivity procedure is to be used in conjunction with a multiobjective optimization procedure suitable for high speed applications. Specifically, the integration of sonic boom and aerodynamic performance criteria in the optimization procedure with the aim of minimizing sonic boom while improving the vehicle's aerodynamic performance will be addressed. The motivation for this choice of the flow problem originates from the fact that such an optimization effort using discrete sensitivity analysis is already underway. Thus the proposed application will serve as a comparison study between the two types of procedures, which is a major objective of the present effort. A brief description of the optimization problem, the associated procedures, the procedure used for evaluating the sonic boom signature and a description of the aerospace vehicle configurations used in the present research effort are given in Appendix A.

2) Parallelization of the Sensitivity Analysis Procedure:

The optimization procedure will need to be efficient from a computational perspective to be of use in practical applications. This is especially important in the present case where a comprehensive CFD solver is coupled with the optimizer. One of the areas to be addressed from the computational efficiency point of view is the sensitivity analysis part of the optimization procedure. For a relatively large number of design variables, the sensitivity analysis may be computationally intensive even in the case of semi-analytical sensitivity analysis (which is superior to finite difference based analysis in terms of computational efficiency). Parallel computing is an area which may be of use in this respect. There has been a lot of interest in parallel computing in recent years. The primary attention has been focused on the CFD solvers which are in use to address flow solutions of large scale practical problems. It has been demonstrated that parallelization allows the distribution of the computational effort over several processors and, hence, can save turn around time of the computational solution codes.

One of the main aims of the proposed work is the parallelization of the sensitivity analysis leading to a more efficient optimization procedure. The sensitivity analysis may be based on finite difference or semi-analytical techniques. Finite difference design sensitivity calculations show coarse grained parallelism and can be easily parallelized since, in addition to the initial flow field solution, one flow field evaluation per design variable must be evaluated in each optimization

cycle. On the other hand, the semi-analytical sensitivity techniques may have fine grained parallelism which requires careful restructuring of the techniques for improved efficiency. Therefore, a study of the parallelization issues associated with the continuous and discrete sensitivity analysis approaches is proposed. This study will mainly address parallelization of the solution techniques for large linear systems of equations which commonly arise in CFD and semi-analytical sensitivity calculations. Established parallelization techniques/algorithms as well as techniques such as *pre-conditioned conjugate gradient* methods will be investigated for efficient parallelization of the sensitivity analysis related equation. One of the key aspects of this effort may be the analysis of parallelization issued associated with the CFD solver itself and importing the relevant ideas for parallelizing the sensitivity analysis. Possible implementation of the semi-analytical techniques in parallel processing environments will be one of the main aims of the proposed work. The following briefly outlines the basic strategy being considered for addressing the parallelization issues associated with the sensitivity analysis procedure.

a) The biggest impact of parallelization will be in the sensitivities calculations. As far as UPS3D, since the solution procedure is that of space marching, one of the ideas is to lag the sensitivities calculation by one plane (i.e. flow solution in n^{th} plane goes on while the sensitivities are calculated in the $(n-1)^{th}$ plane using the already solved flow variables (from previous step). For example, the flow field is represented by the set of equations in the form

$$\mathbf{A}\varphi = \mathbf{R}$$

where φ is the flow variables vector. Similarly, the corresponding equations for the sensitivities are represented by

$$\mathbf{B}\theta_i = \underline{\mathbf{R}}_i$$

where θ_i is the sensitivity vector corresponding to the design variable ϕ_i The proposed effort in this case corresponds to solving the above two sets of equation in parallel with the latter equation(s) lagged by one plane from the former. This would enable time savings of the order of what it takes to compute either the flow or the sensitivities (whichever is faster). One of the foreseeable penalties is that an extra plane of flow variables will have to be stored.

b) Since the individual sensitivities are independent of each other (represented by the second set of equations above), they can all be solved in parallel. Since the equations to be solved all have the same structure, the same numerical algorithm (with different coefficients) can be used. The structure of the equation set representing the flow field is similar to the sensitivity equations and so the numerical algorithm used for evaluating the flow field will be useful here. The overall savings from the above two parts ((a) & (b)) could be 25% over and above the savings associated with using the analytical sensitivities instead of finite difference sensitivities.

c) Parallelizing UPS3D:- It is proposed to address the subroutines that directly affect the sensitivities calculations (semi-analytical & continuous) first. Large scale matrix operations benefit tremendously from parallel computational algorithms. The UPS3D code includes many subroutines which involve such matrix manipulations (e.g.. THOMAS, BMAT, BTRI etc.). These may become computationally more efficient if they are parallelized. We will work closely with the NASA Ames personnel in this regard.

Deliverable:

1) A comparative study of discrete and continuous semi-analytical sensitivity analysis techniques will be done. The accuracy and computational efficiency of the two techniques will be compared using representative model optimization problems. The nature of the optimum solutions and the computational efficiency will also be analyzed.
2) Parallelization of the sensitivity analysis procedure will be initiated. Initially, the modules that are used to evaluate the sensitivities will be modified to be used in a parallel mode along with the flow field solution module. Subsequently, the issue of parallelizing individual subroutines that directly affect the sensitivity analysis will be addressed.

Appendix A

In order to validate the developed sensitivity techniques, it is proposed to study their performance in three-dimensional, single-point optimization problems with different sets of objective functions and constraints such as drag coefficient, C_D, lift coefficient, C_L, C_L/C_D ratio, and wing weight, W. Problems from high subsonic and transonic flight regimes will be considered in the validation study.

Optimization Problem:

The optimization problem involves multiple objectives and constraints and can be stated as follows.

Minimize

Δp_{max} and C_D/C_L

subject to the constraints

$$C_{Lmin} \leq C_L \leq C_{Lmax}$$

$$\Phi_{min} \leq \Phi \leq \Phi_{max}$$

where Δp_{max} is the first peak in the overpressure signal at a specified distance from the aircraft, C_D/C_L is the drag to lift ratio, Φ is the design variable vector and the subscripts "min" and "max" denote lower and upper bounds respectively. Upper and lower bounds are imposed on the design variables during the optimization to prevent unrealistic results. All the design variables that will allow a comprehensive investigation of their individual effects on the overall performance of the aircraft, must be included in the optimization problem.

Since the above optimization problem involves multiple design objectives (two in the present case), traditional optimization techniques which typically consider a single objective function, cannot be used. In the present work, a multiobjective function formulation, based on the Kreisselmeier-Steinhauser (K-S) function approach [1], has been used. This approach is described next.

Kreisselmeier-Steinhauser (K-S) Multiobjective Formulation

The K-S function approach helps combine the multiple objective functions and the design constraints into a single composite envelope function which is then minimized using unconstrained techniques. The first step in forming the composite objective function involves the transformation of the original objective functions into reduced objective functions [1]. These reduced objective functions assume the form,

$$F_k^*(\Phi) = 1.0 - \frac{F_k(\Phi)}{F_{k_o}} - g_{max} \leq 0 \qquad k = 1, \ldots, NOBJ \tag{A-1}$$

where F_{k_o} represents the value of the original objective function F_k, calculated at the beginning of each optimization cycle. NOBJ denotes the total number of objective functions in the original

optimization problem. The quantity g_{max} is the value of the largest constraint of the original optimization problem and is held constant during each cycle. Since the reduced objective functions assume the form of constraints, a new constraint vector $f_m(\Phi)$ (m = 1, 2, ... , NCON+NOBJ, where NCON is the total number of constraints in the original optimization problem) is introduced. The constraint vector includes the original constraints and the constraints introduced by the reduced objective functions (Eq. A-1). The new objective function to be minimized is then defined using the K-S function as follows.

$$F_{KS}(\Phi) = f_{max} + \frac{1}{\rho}\log_e \sum_{m=1}^{M} e^{\rho(f_m(\Phi)-f_{max})} \qquad \text{(A-2)}$$

where f_{max} is the largest constraint corresponding to the new constraint vector $f_m(\Phi)$ (in general not equal to g_{max}). When the original constraints are satisfied during optimization, the constraints due to the reduced objective functions are violated. Initially, in an infeasible design space, where the original constraints are violated, the constraints due to the reduced objective functions (Eqn. A-1) are satisfied (i.e. g_{max} is negative). The optimizer attempts to satisfy these violated constraints thus optimizing the original objective functions (F_k). The multiplier ρ, which is analogous to the draw-down factor of penalty function formulation, controls the distance from the surface of the K-S envelope to the surface of the maximum constraint function (Fig. 1). When ρ is large, the K-S function will closely follow the surface of the largest constraint function and when ρ is small, the K-S function will include contributions from all violated constraints with equal weight.

The new unconstrained optimization problem can be solved by using a variety of techniques. In the present work, it is solved using the Broyden-Fletcher-Goldfarb-Shanno (BFGS) algorithm [2]. This algorithm approximates the inverse of the Hessian of the composite objective function using a rank-two update and guarantees both symmetry and positive definiteness of the updated inverse Hessian matrix.

Approximation Technique

During the optimization, several evaluations of the objective functions and the constraints need to be done in each optimization cycle. The use of exact analysis to evaluate them at each iteration during an optimization cycle is computationally expensive. Therefore, an approximation technique known as the two-point exponential approximation [3], is used within the optimizer for approximating the objective functions and the constraints. This technique utilizes the gradient of the function with respect to design variables from the current and previous design cycles and is formulated as follows.

$$\hat{F}(\Phi) = F(\Phi_1) + \sum_{n=1}^{NDV}\left[\left(\frac{\phi_n}{\phi_{1n}}\right)^{p_n} - 1.0\right]\frac{\phi_{1n}}{p_n}\frac{\partial F}{\partial \phi_n}(\Phi_1) \qquad \text{(A-3)}$$

where $\hat{F}(\Phi)$ is the approximation of the function $F(\Phi)$ in the neighborhood of the current design variable vector, Φ_1. The quantity ϕ_n is the n^{th} design variable from the design variable vector Φ. NDV is the total number of design variables. The approximate values for the constraints, $\hat{g}_{j(}\Phi)$, are similarly calculated. The exponent p_n is defined as

$$p_n = \frac{\log_e\left\{\left[\frac{\partial F}{\partial \phi_n}(\Phi_o)\right] \Big/ \left[\frac{\partial F}{\partial \phi_n}(\Phi_1)\right]\right\}}{\log_e\left\{\left[\frac{\Phi_{on}}{\Phi_{1n}}\right]\right\}} + 1.0 \qquad \text{(A-4)}$$

where Φ_1 refers to the design variable vector from the current cycle and Φ_0 denotes the design variable vector from the previous cycle. Equation A-1 indicates that in the limiting case of $p_n = 1$, the expansion is identical to the traditional first order Taylor series and when $p_n = -1$, the two-point exponential approximation reduces to the reciprocal expansion form. Therefore, the exponent (p_n) can be interpreted as a "goodness of fit" parameter which explicitly determines the trade-off between traditional and reciprocal Taylor series based expansions. p_n is chosen to be within the interval, $-1 \le p_n \le 1$ thus resulting in a hybrid approximation technique.

Sonic Boom Analysis:

The CFD based analysis procedure for evaluating sonic boom is described in this section. For isentropic flow past smooth axisymmetric bodies, the pressure disturbances (sonic boom) at large distances from the aircraft can be evaluated by using the Whitham F-function [4], which is based on the Abel integral of the equivalent area distribution of the aircraft. Lighthill [5] developed an alternate formulation of the F-function which was shown to be suitable for sonic boom prediction of smooth and non smooth projectile shapes. Walkden extended Whitham's theory [6] for application to wing-body configurations. The asymptotic form of the equations used in developing the sonic boom overpressure signature ($\Delta p/p_\infty$), is as follows.

$$\frac{\Delta p}{p_\infty} = \gamma M_\infty^2 F(y) / \sqrt{2\beta d_o} \qquad \text{(A-5)}$$

$$x = y + \beta d_o - \kappa\sqrt{d_o} F(y) \qquad \text{(A-6)}$$

$$\beta = (M_\infty{}^2 - 1)^{0.5} \qquad \text{(A-7)}$$

$$\kappa = (\gamma + 1) M_\infty{}^4 / [\beta * (2\beta)^{0.5}] \qquad \text{(A-8)}$$

$$\Delta p = (p_{local} - p_\infty), \qquad \text{(A-9)}$$

where F(y) is the Whitham F-function, $\gamma = 1.4$ for air and M_∞ is the free stream Mach number. The equation, $y(x, d_o)$ = constant, is a characteristic curve, x is the streamwise distance and d_o is a specified distance from the flight axis. Since the above mentioned models are based on linearized theory, they fail to agree with wind-tunnel data in highly nonlinear flows such as the flow at angle-

of-attack at high Mach numbers ($M_\infty > 2$). Hicks and Mendoza [7] have developed a technique to extrapolate the pressure signature at d_o to a distance d_1 ($d_1 > d_o$). First, a pressure signature at distance d_o, where the flow field is assumed to be locally axisymmetric, is directly measured in the wind-tunnel and the value of the F-function (at d_o) is evaluated. Since the pressure signal propagates at the local speed of sound and each point of the signal advances according to its amplitude, the signal is distorted as it propagates away from the aircraft and the F-function becomes multivalued. The new F-function at d_1 is obtained by placing discontinuities (shocks) in such a way that the discontinuities divide the multivalued regions with equal areas on either side of them. This new F-function gives the overpressure signature at d_1 using Eqs. (A-5) and (A-6).

Cheung et al. [8] have used a three-dimensional parabolized Navier-Stokes (PNS) code in combination with Whitham's quasilinear theory for sonic boom prediction. The CFD code used in this study, UPS3D, solves the PNS equations governing the flow using an implicit, approximately factored, finite volume algorithm [9]. The flow field associated with wing-body configurations is evaluated and the drag, lift and moment coefficients are computed. Three different approaches have been used by Cheung et al. to obtain the overpressure signal at mid- and far-fields from the near-field CFD solution. One of these three approaches is based on the extrapolation technique described above. In the present work, this extrapolation procedure is used in conjunction with the UPS3D code, to evaluate the sonic boom pressure signatures.

Aircraft Configuration:

The developed optimization procedure is applied to two different aircraft configurations. The first one, illustrated in Fig. 2, is a delta wing-body configuration and the second one, illustrated in Fig. 3, is a doubly swept wing-body configuration. In both configurations, the centerbody is axisymmetric and is a combination of a nose region and an extended cylindrical region. In the nose region, the radius of the centerbody varies parabolically with the streamwise coordinate over the nose length. The radius of the cylinder is denoted r_m. In the nose region, the radius of the body changes from zero (at the tip) to r_m over a nose length, l_n, as follows.

$$r = r_m - r_m*(1 - x/l_n)^2 \qquad \text{(A-10)}$$

Here x is the streamwise distance measured from the nose tip. For the first configuration considered (Fig. 2), the wing planform is delta shaped with a leading edge sweep λ, root chord c_o and wing span w_s. The wing cross section is a symmetric, diamond airfoil (Fig. 2) whose maximum thickness-to-chord ratio is denoted t_c. For the second configuration, the wing planform is characterized by a double sweep with sweep angles λ_1 and λ_2 and a break length, x_b (Fig. 3). The wing root chord is denoted c_o and tip chord is denoted c_t. The wing cross section is a diamond airfoil with thickness-to-chord ratio, t_c. For both configurations, the total body length is denoted l_b and the wing starting location is denoted x_w.

For the delta wing-body configuration case, the leading edge sweep (λ), the wing root chord (c_o), the wing span (w_s), the airfoil thickness-to-chord ratio (t_c), the maximum nose radius (r_m) and the nose length (l_n) are used as design variables. For the doubly swept wing-body configuration case, the two leading edge sweeps (λ_1 and λ_2), the break length (x_b), the wing root chord (c_o), the wing tip chord (c_t), the maximum nose radius (r_m), the nose length (l_n) and the wing starting location (x_w) are used as design variables.

Discrete Semi-analytical Sensitivity Analysis

In general, an aerodynamic performance coefficient, C_j, depends on the steady-state flow variables, Q^*, the vector of computational grid coordinates, X, and, sometimes, explicitly on the vector of independent design variables, ϕ. Mathematically,

$$C_j = C_j(Q^*(\phi), X(\phi), \phi) \tag{A-11}$$

The derivative of C_j with respect to the i^{th} design variable, ϕ_i, is given by,

$$\frac{dC_j}{d\phi_i} = \left\{\frac{\partial C_j}{\partial Q^*}\right\}^T \left\{\frac{\partial Q^*}{\partial \phi_i}\right\} + \left\{\frac{\partial C_j}{\partial X}\right\}^T \left\{\frac{\partial X}{\partial \phi_i}\right\} + \frac{\partial C_j}{\partial \phi_i} \tag{A-12}$$

In Eqn. A-12, the terms $\left\{\frac{\partial C_j}{\partial Q^*}\right\}$, $\left\{\frac{\partial C_j}{\partial X}\right\}$ and $\frac{\partial C_j}{\partial \phi_i}$ are easily calculated knowing the explicit dependence of C_j on Q^*, X and ϕ_i. The term $\left\{\frac{\partial Q^*}{\partial \phi_i}\right\}$, which represents the sensitivity of the steady state flow variables with respect to the i^{th} design variable, is calculated using the direct differentiation technique. In the discrete sensitivity approach, the discretized flow equations are directly differentiated, as described here. The discretized flow equations which model the flow can be written as follows.

$$\{R(Q^*(\phi), X(\phi), \phi)\} = \{0\} \tag{A-13}$$

Equation A-13, differentiated with respect to ϕ_i, gives

$$\left\{\frac{dR}{d\phi_i}\right\} = \left\{\frac{\partial R}{\partial Q^*}\right\}^T \left\{\frac{\partial Q^*}{\partial \phi_i}\right\} + \left\{\frac{\partial R}{\partial X}\right\}^T \left\{\frac{\partial X}{\partial \phi_i}\right\} + \frac{\partial R}{\partial \phi_i} = \{0\} \tag{A-14}$$

Equation A-14 represents a set of linear algebraic equations in $\frac{\partial Q^*}{\partial \phi_i}$ which can be solved easily. It is to be noted that the terms $\left\{\frac{\partial R}{\partial Q^*}\right\}$, $\left\{\frac{\partial R}{\partial X}\right\}$ and $\frac{\partial R}{\partial \phi_i}$ in Eqn. A-14, can be calculated easily, knowing the explicit dependence of {R} on Q^*, X and ϕ_i. References 10 and 11 illustrate the use of the discrete sensitivity analysis techniques for design optimization of high speed vehicle configurations to obtain the configurations corresponding to minimum sonic boom and improved aerodynamic performance.

REFERENCES

1. Kreisselmeier, A. and Steinhauser, R., "Systematic Control Design by Optimizing a Vector Performance Index," *Proceedings of the IFAC Symposium on Computer Aided Design of Control Systems*, Zurich, Switzerland, 1979, pp. 113-117.
2. Haftka, R. T., Gurdal, Z. and Kamat, M. P., "Elements of Structural Optimization," *Kluwer Academic Publishers*, Dordrecht, The Netherlands, 1990.
3. Fadel, G. M., Riley, M. F. and Barthelemy, J. F. M., "Two-Point Exponential Approximation Method for Structural Optimization," *Structural Optimization, 2*, 1990, pp. 117-124.
4. Whitham, G. B., "The Flow Pattern of a Supersonic Projectile," *Communications on Pure and Applied Mathematics*, Vol. 5, No. 3, 1952, pp. 301-348.
5. Lighthill, M. J., "General Theory of High Speed Aerodynamics, Sec. E; see also High Speed Aerodynamics and Propulsion," Vol. 6, Princeton University Press, NJ, 1954, pp. 345-389.
6. Walkden, F., "The Shock Pattern of a Wing-Body Combination, Far from the Flight Path," *Aeronautical Quarterly*, Vol. 9, Pt. 2, May 1958, pp. 164-194.
7. Hicks, R. and Mendoza, J., "Prediction of Aircraft Sonic Boom Characteristics from Experimental Near-Field Results," *NASA TMX-1477*, November, 1967.
8. Cheung, S. H., Edwards, T. A. and Lawrence, S. L., "Application of Computational Fluid Dynamics to Sonic Boom Near- and Mid-Field Prediction," *Journal of Aircraft*, Vol. 29, No. 2, 1992, pp. 920-926.
9. Lawrence, S., Chaussee, D. and Tannehill, J., "Application of an Upwind Algorithm to the 3-D Parabolized Navier-Stokes Equations," AIAA Paper 87-1112, June 1987.
10. Narayan, J. R., Chattopadhyay, A., Pagaldipti, N. and Cheung, S. H., "Optimization Procedure for Improved Sonic Boom and Aerodynamic Performance Using a Multiobjective Formulation Technique," AIAA Paper 95-0127, *33rd Aerospace Sciences Meeting and Exhibit*, Reno, Nevada, January 1995.
11. Chattopadhyay, A., Narayan, J. R., Pagaldipti, N., Xu, W. and Cheung, S. H., "Optimization Procedure for Reduced Sonic Boom in High Speed Flight," AIAA Paper 95-2156, *26th AIAA Fluid Dynamics Conference*, San Diego, California, June, 1995.

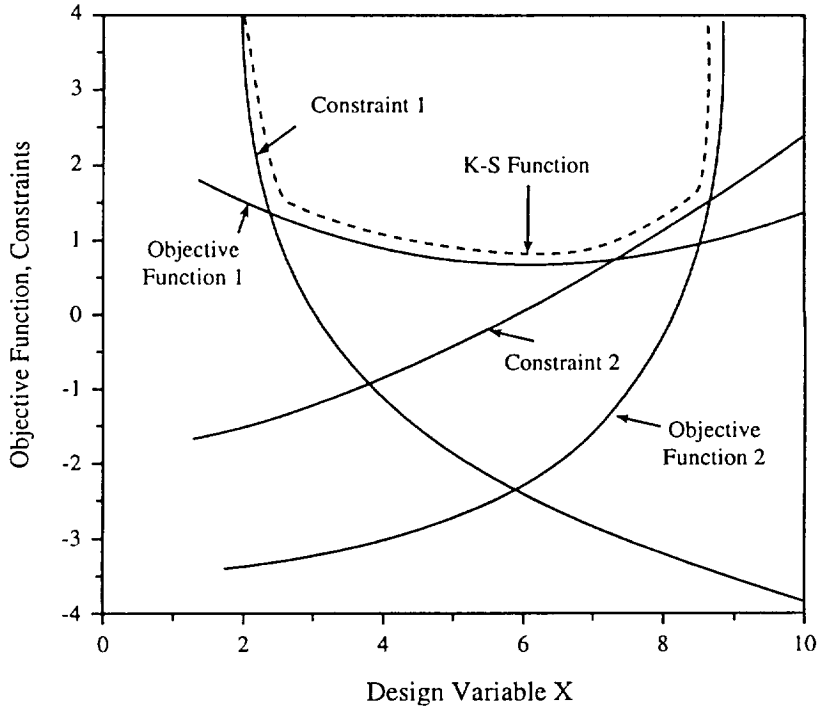

Figure 1. Kreisselmeier-Steinhauser function envelope

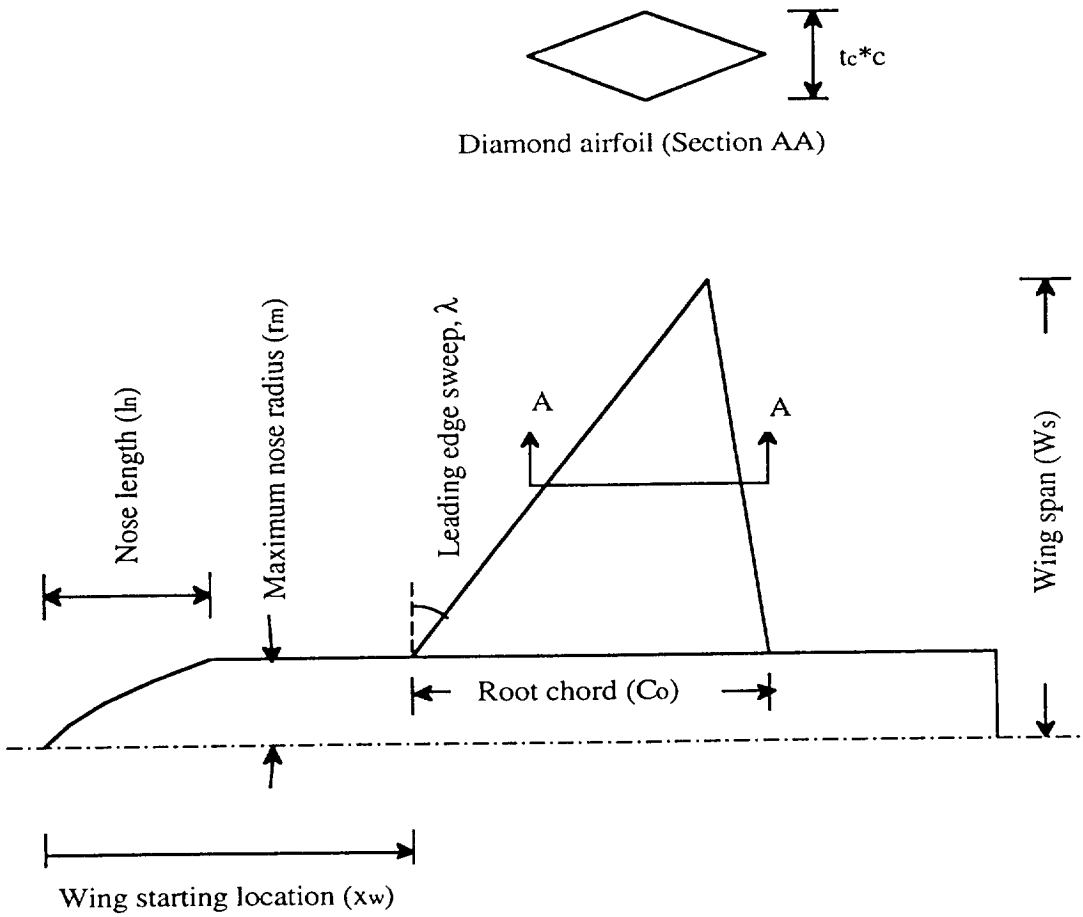

Figure 2. Design variables for the delta wing-body configuration

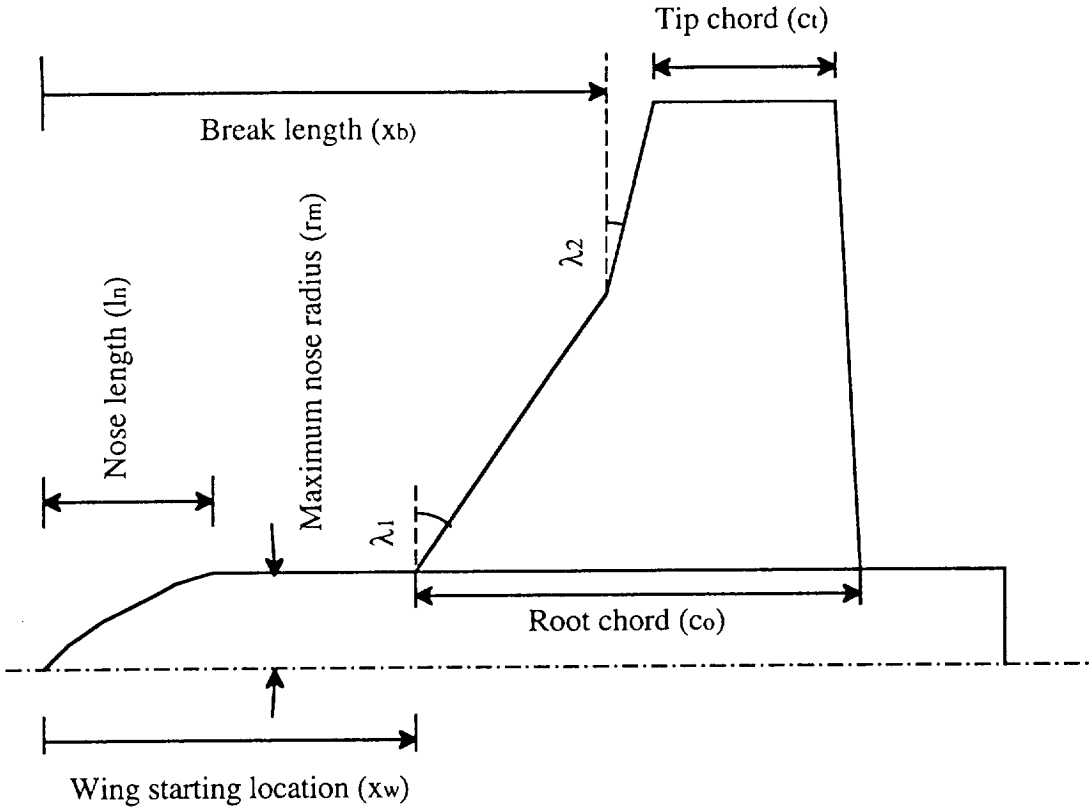

Figure 3. Double sweep wing-body configuration